Available online at www.sciencedirect.com
SCIENCE DIRECT
Carbohydrate Research 340 (2005) 2752–2760
Carbohydrate RESEARCH

Conformational analysis of xylan chains

Karim Mazeau,[a,*] Charlotte Moine,[b] Pierre Krausz[b] and Vincent Gloaguen[b]

[a]*Centre de Recherches sur les Macromolécules Végétales (CERMAV-CNRS, UPR 5301, and Université Joseph Fourier-Grenoble 1, ICMG, FR2607), BP 53, F-38041 Grenoble, France*
[b]*Laboratoire de Chimie des Substances Naturelles, Faculté des Sciences et Techniques, Université de Limoges, 123 rue A. Thomas, Limoges, France*

Received 24 June 2005; received in revised form 27 September 2005; accepted 29 September 2005
Available online 10 November 2005

Abstract—The present study provides a theoretical description of the different levels of structural organization that characterize the xylan polysaccharide in its native and hydrophobic lauroyl esterified forms. The goal of this study was to ascertain the role played by the hydroxyl or lauroyl side groups on the conformational flexibility of the xylan chain backbone. The results reported provide a detailed description of the low-energy conformers of the dimer segments, a complete characterization of the helical structures, an insight into the disordered state of the polysaccharide chains and an estimation of the cohesion of the amorphous solids. Esterification of xylan hydroxyl groups by lauric acid has a large effect on the conformational properties of the glycosidic bonds linking two repeat units. Both the location and the relative energies of the low energy areas of the potential energy surfaces strongly differ: extended and coiled conformations are preferred for the native and hydrophobic forms, respectively. Consequently, the predicted unperturbed polymer chain extension strongly depends on the structure, predicted L_p of the native xylan of 35 Å compares favourably well with the experimental ones, this characteristic dramatically decreases to 9 Å for the hydrophobically modified chain. Curiously, only extended 2_1 and left-handed 3_1 helical structures are calculated stable for both polymers. The estimated cohesive parameters of amorphous bulks reveal that inter-chain interactions are stronger for the xylan chain than that for modified one, the former being stabilized by hydrogen bonds whereas hydrophobic interactions play a determinant role for the latter.

Keywords: Xylan; Conformational analysis; Molecular modeling; Potential energy surface; Helix; Persistence length; Amorphous solid

1. Introduction

Xylans are the most common hemicelluloses of the plant kingdom. They represent 20–30% (dry weight) of wood and up to 50% (dry weight) of some cereal seeds. In the current trend for a complex and effective utilization of biomass, increasing attention has been paid during the last few years to the exploitation of xylans as biopolymer resources.[1,2] To this end, thermoplastic films were obtained from modified plant cell wall polysaccharides by grafting their hydroxyl groups with hydrophobic fatty acid chains. A direct relation exists between the substitution of an esterified polysaccharide and the mechanical behaviour of the resulting plastic film.[3] This behaviour can be accounted for by the fatty acid. We recently proposed an easy and rapid method to perform direct homogeneous acylation of hemicelluloses by lauroyl chloride,[4] giving rise to highly hydrophobic esterified products, in contrast to natural hemicelluloses which are usually hydrophilic. This increased lipophilicity is in agreement with their use as thermoplastic materials or films for packaging. Lauroyl-derived xylan films revealed a rather poor extension at break (10.5%) but a relatively high tensile strength (7.1 MPa); both parameters, which express the film stretching ability and the resistance to traction, respectively, are in accordance with some values observed with other plastified carbohydrate biopolymers.[5–7] The elastic modulus E (332 MPa) which measures the intrinsic stiffness of the plastic film was close to those of commercial products,

* Corresponding author. Tel.: +33 4 76 03 76 39; fax: +33 4 76 54 72 03; e-mail: karim.mazeau@cermav.cnrs.fr

0008-6215/$ - see front matter © 2005 Elsevier Ltd. All rights reserved.
doi:10.1016/j.carres.2005.09.023

such as polyethylene film. In addition, the thermomechanical properties of the dodecyl-grafted xylan film revealed a glass transition temperature (T_g) of 133 °C, which is lower than that of the parent polymer ($T_g = 180$ °C),[8] the lowering of T_g of xylan ester is due to both a decrease in polymer–polymer interactions and to an increase in free volume as fatty chains are introduced.

The physico-chemical and functional properties of the xylan chains in their native and modified forms depend on the intrinsic conformational behaviour of the individual chains together with their ability to interact in the condensed state. A detailed knowledge of such fundamental properties is required in order to achieve a more rational use of this resource. Thus far, only rigid conformational samplings of xylobiose, based on very simple potential functions have been reported,[9,10] the state of the art of the modelling of oligosaccharide structures in isolation uses the relaxed and adiabatic grid search sampling strategy, coupled with MM3, a robust and sophisticated method to estimate the energies of the different conformations of the system.

Owing to their botanic origin, xylan displays a large variety and a baffling structural complexity.[11] In terrestrial plants, the linear β-(1→4)-D-xylopyranan backbone is substituted by a variety of different side chains, mainly, single α-L-arabinofuranosyl and α-D-glucopyranosyl uronic acid (along with its 4-*O*-methyl ether) units. In addition, rhamnose, xylose, galactose, glucose next to acetyl groups and phenolic acids have been identified. In this study, only homo-xylan chains are considered, the effects of substituents will be further investigated. The aim is to characterize and compare the conformational behaviours of native and fully lauroyl-esterified xylan chains.

2. Material and methods

Models studied here consist of a single (1→4)-linked β-D-xylopyranose repeating unit. The schematic representation of the dimer repeat units are displayed in Figure 1. The two disaccharides (**Xyl-Xyl** and **Xyl23s-Xyl23s**) represent the extreme combinations of the primary structures that occur in this polymer in its native and lauroyl modified forms. **Xyl-Xyl** represents the unsubstituted polymer and to investigate how the presence of the side chains influence the conformational flexibility of the chain, we also considered the fully substituted structure **Xyl23s-Xyl23s**.

2.1. Force fields

Two different force fields were used in this study. Calculations on isolated molecules (dimers and helices) were performed using the molecular mechanics program MM3(92).[12,13] MM3 has been shown to be well adapted to model carbohydrate structures as this force field contains a correction for anomeric effect. The block-diagonal minimization method, with the default energy convergence criterion of $0.00008 * n$ kcal mol^{-1} per five iterations, n being the number of atoms, was used for optimizations.

In contrast, to model dense solids, we used the second-generation force-field PCFF[14–18] specially suited for polymers and other materials. The PCFF force field

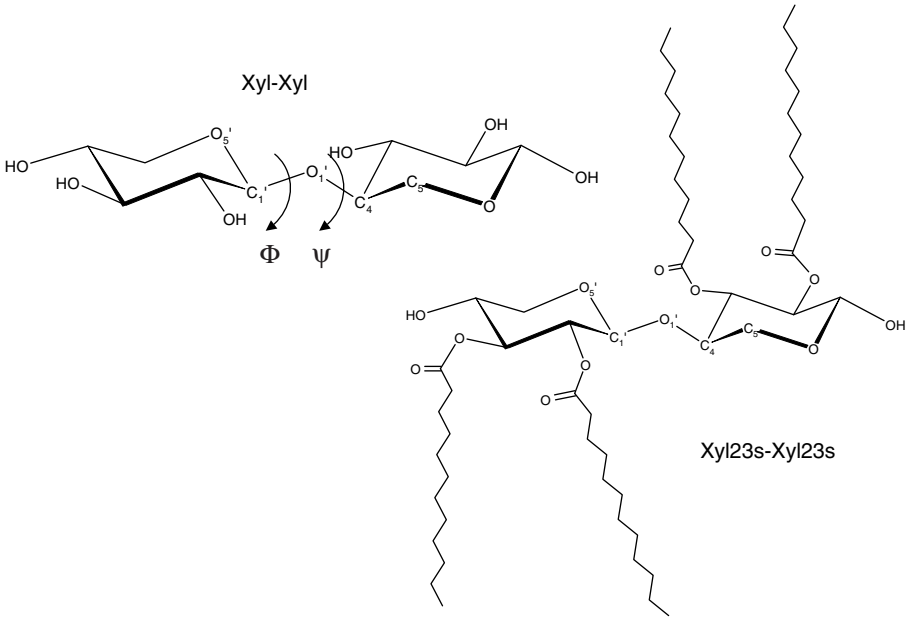

Figure 1. Schematic representation of the two disaccharides: **Xyl-Xyl** and **Xyl23s-Xyl23s**. The ϕ and ψ torsion angles of interest are also included.

is an improved version of the consistent force field (CFF91) for which new functional groups were added. The CFF91 force field have been parameterized and validated using condensed phase properties in addition to various ab initio and empirical data for molecules in isolation. This force field was successfully used to model bulks of cellulose in the amorphous and crystalline states.[19]

A dielectric constant, $\varepsilon = 4$, was used in all the calculations.

2.2. Monomeric units

Only the stable chair $^4C_1$ conformation has been considered for the pyranoid rings. Each residue has been built from standard crystallographic values of the bond lengths and bond angles internal geometrical parameters. Each residue was then subjected to an optimization through the force field in use.

2.3. Glycosidic linkages

The conformations around the glycosidic linkages of all the dimeric fragments constituting the polysaccharide should first be carefully established to properly describe the conformations of the polymer chain. As a general rule in the conformational analysis of carbohydrates, the global shape of a disaccharide is mainly governed by the rotations about the glycosidic linkages.[20] The relative orientations of the two saccharide units are expressed in terms of the glycosidic linkage torsion angles ϕ and ψ: $\Phi =$ O-5′–C-1′–O-1′–C-4; $\Psi =$ C-1′–O-1′–C-4–C-5. The conformational space of each segment was explored in a systematic manner by stepping the glycosidic ϕ and ψ torsion angles in 20° increments over the whole angular range. At each conformational microstate, a geometry optimization was performed by allowing coordinates of each atom to vary, except those defining the ϕ and ψ torsion angles.

Several different conformations and orientations of the pendant groups were considered as starting geometry to calculate relaxed conformational maps. A Monte-Carlo protocol was used to randomly generate many staggered orientations of the pendant O-2′, O-3′, O-4′, O-1, O-2 and O-3 hydroxyl groups of the **Xyl-Xyl** disaccharide. The same procedure was applied to the O-4′, O-1 hydroxyls and the lauroyl chains at positions 2, 3, 2′ and 3′ for the **Xyl23s-Xyl23s**. Adiabatic contour maps were then drawn for the two disaccharides in which only the lowest energy conformer at each (ϕ, ψ) point is used for Ramachandran-like contour plots. The adiabatic procedure has the advantage of overcoming the well-known multiple-minima problem of the potential energy hypersurface due to specific orientations of the pendant groups and of fully describing the conformational flexibility around glycosidic linkages.

2.4. Generation of helices

From the geometries of different minima found by the MM3 grid searches, regular helices were generated using the polysaccharide builder program POLYS.[21] Helices are characterized by the two helical parameters n and h; n being the number of repeating units per turn of helix and h the projection of a repeating unit on the helical axis. To build helices, POLYS requires the geometry of the different monosaccharide units and the torsion angles (ϕ, ψ) as inputs. The monosaccharides used here come from the preliminary study of disaccharides and were then implemented in the MONOBANK.[22] Regular helices are obtained in a three-step procedure: (1) the program calculates the helical parameters (n, h) from (ϕ, ψ) values which correspond to the different minima of disaccharide potential energy surfaces; (2) these values are adjusted to give the nearest n-fold helical structure, that is, an integral value of n; (3) regular helices are finally built using the adjusted (ϕ, ψ) values. Such regular helices were generated for the native and modified main chain containing nine repeating units. The structures were then minimized by MM3 in order to relax any possible bad contact created during step 2 of the POLYS procedure. A short molecular dynamics run was then performed on the modified fragment in order to allow the lauroyl chains to find their optimal geometry; to maintain the helical characteristics of the whole chain, the coordinates of the backbone atoms were constrained.

2.5. Random conformations of the chain

The generation of chains in random conformation and containing a high number of glycosyl units allows the calculation of chain dimensions in the unperturbed state.[23] For this purpose, a Metropolis algorithm[24] of the Monte-Carlo technique (the in-house program METROPOL[25]) was used to generate a large sample of polymer conformations, distributed according to Boltzmann statistics, and to calculate the corresponding characteristics of chains. Starting from the coordinates of the disaccharide, the chain was constructed step by step, by addition of a new residue described by the (ϕ, ψ) couple randomly selected. The new conformation, represented by the (ϕ, ψ) couple, is tested on an energy criterion: the energy difference ΔE between the newly generated state and the previous one is calculated. If the new state has an equal or lower energy, the (ϕ, ψ) couple is accepted; otherwise a Metropolis test is applied. The test generates a random number between 0 and 1 and compares it to the Boltzmann factor $e^{-\Delta E/RT}$; if it is smaller, the state is accepted; otherwise it is discarded and a new couple is selected.

The unperturbed average dimensions of the chains[26] were evaluated from five independent statistical samples

of 4000 polymer chains having 1000 residues, at 298 K. The polymer average size is related to the persistence length L_p as a function of the polymerization degree n; it is defined as the projection of the end-to-end distance vector **r** on the first bond of the chain and represents an estimation of the length through which the propagation of the chain in a given direction is preserved. Reproducible results were obtained with average deviations lower than 2%.

2.6. Amorphous solids

The amorphous bulk of the polymer is modelled by periodic cubic microstructures. The first repeat unit is filled into the box by choosing place and orientation at random. Then, a random conformation of a polymer is built one residue at a time within the cell. A conformation is accepted if the generated residue is free of strong steric clashes with all the previously generated ones. As segments were added to the growing chain, the nonbond distances of the conformation generated were checked. To facilitate the generation of the polymer within the box, a scale factor of 0.3 was applied to all the van der Waals interactions in this first stage of the generation. The minimum nonbond distance allowed is equal to the sum of the two atom's van der Waals radii multiplied by this specified scale factor. As results on cellulose[19] have been shown to be independent on both the initial chain length and the initial density, we have used a unique chain of DP 50 and the initial density was set to 1.25 g/cm^3. An amorphous ensemble containing ten independent conformations is constructed.

Each amorphous structure should correspond to an energy minimum of the potential energy and second it should be free of internal tension or compression. The generated structures are then equilibrated by performing several relaxation cycles. Each relaxation cycle consists in a first energy minimization, followed by a 5 ps NVT dynamics run in which the temperature is maintained at 800 K, followed by an energy minimization, 20 ps NVT at 600 K, minimization. Then another 20 ps dynamics at 400 K was performed in the NPT ensemble in which the simulation box was allowed to vary in size and shape. This was again followed by a final energy minimization.

Minimizations were performed by both steepest descent and conjugated gradient methods; the convergence criteria used was a root-mean-square (rms) force less than 0.1 (kcal/mol)/Å for the polymer and 0.1 (kcal/mol)/Å^3 for the stresses on the periodic boxes. Both convergence criteria were simultaneously satisfied for the system to be relaxed completely.

For the molecular dynamics simulations, the standard Verlet[27] algorithm was used to integrate Newton's law of motion with a time step of 0.001 ps. For the canonical N,P,T dynamics,[28] the relaxation time constant and the mass-like parameter which determines the rate of change of volume/shape matrix were set to 0.1 ps and 1.00, respectively. Each molecular dynamics run was started by assigning initial velocity for the atoms according to a Boltzmann distribution at $2 * T$, T being the target temperature. The velocities of the atoms were quickly scaled down so that the final temperature of atoms was T. The total external pressure was maintained at 1 atm, and Nose's algorithm[29] was used to keep the cell temperature constant.

The simulated structures satisfy the criterion that the values of the components of the internal stress tensor; defined as the first derivatives of the potential energy per unit volume with respect to strains internal stresses, are (close to) zero, which means that the structure being at a local minimum of the potential energy surface and ensures a mechanical equilibrium state.

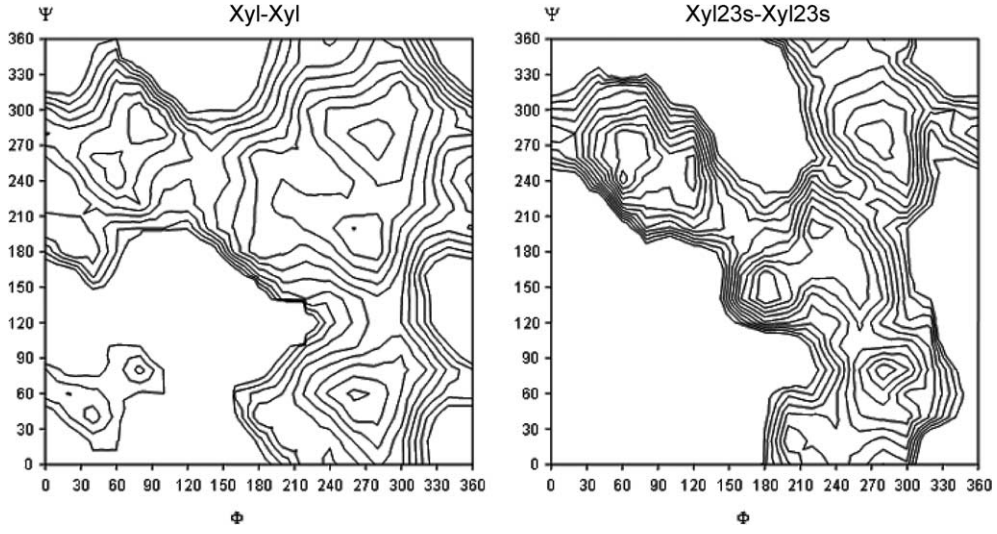

Figure 2. Relaxed conformational energy maps for the two disaccharides calculated using the MM3 force field.

All calculations were performed on a network of Silicon Graphics workstations at the 'Centre d'Expérimentation et de Calcul Intensif', CECIC, Grenoble.

3. Results and discussion

3.1. Flexibility of the glycosidic bonds: potential energy surfaces

The calculated adiabatic conformational energy surfaces (ϕ, ψ) for isolated dimers of native and modified xylans are presented as potential energy contour maps in Figure 2. The contours are separated by 1 kcal mol^{-1} and range from 1 to 10 kcal mol^{-1}. The energies are given relative to the lowest minimum. Geometries and relative potential energies of the predicted minima are listed in Table 1 and the three lowest energy conformers for each compound are shown in Figure 3.

3.1.1. Unsubstituted disaccharide: xylobiose. Adiabatic map of xylobiose, which represents the repeat unit of the native polysaccharide, have been established first. The surface exhibits four wells (Fig. 2). The ϕ, ψ angles of the lowest energy region explore *gauche*-orientations, and the corresponding conformations are extended as those found in the crystal structures of xylans[9,10,30,31] and related polysaccharides. The other regions at (*gauche*−, *gauche*+) and (*gauche*+, *gauche*−) correspond to folded conformations. The three first energy minima are displayed in Figure 3 left, all are stabilized by interresidue hydrogen bonds between C-3 and

Table 1. Torsion angle values (°) across the glycosidic bonds, MM3 relative energies (kcal mol^{-1}), of the different minima of the disaccharides

Disaccharide	Minima	ϕ (degree)	ψ (degree)	ΔE (kcal mol^{-1})
Xyl-Xyl	1	280	280	0.00
	2	260	200	0.51
	3	260	60	1.28
	4	60	240	2.81
	5	80	300	2.82
Xyl23s-Xyl23s	1	60	240	0.00
	2	180	140	0.50
	3	280	80	0.57
	4	220	200	1.80
	5	120	240	2.09
	6	280	280	2.86

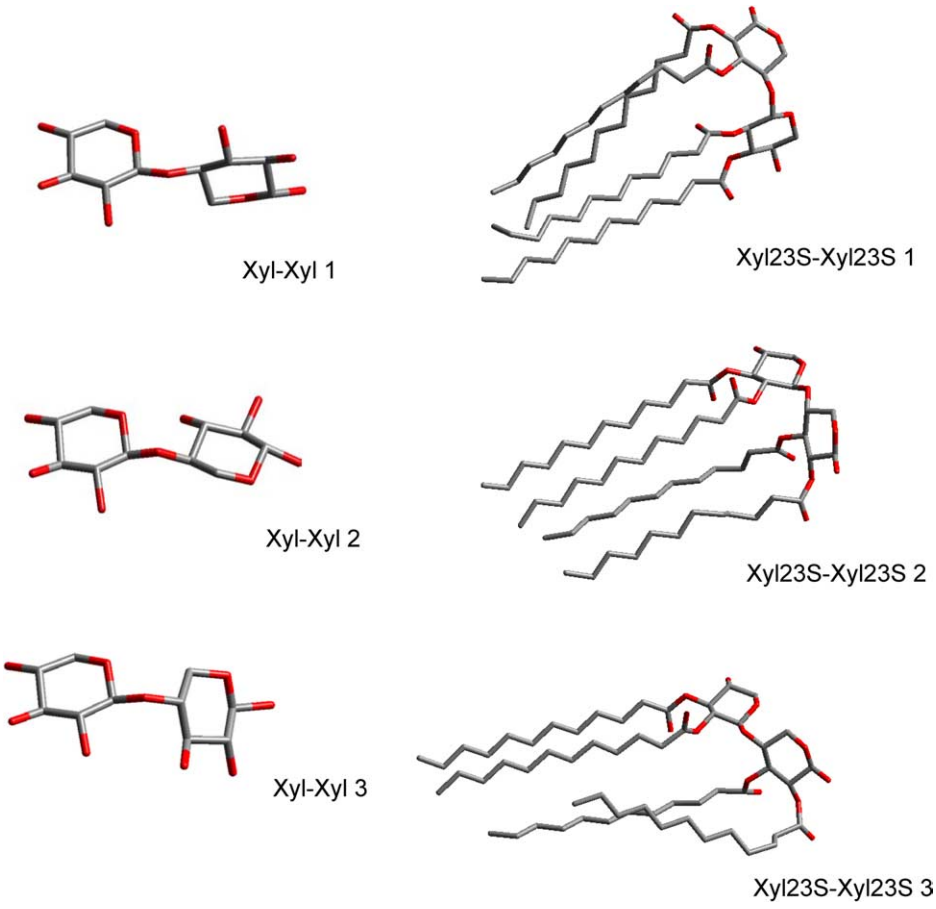

Figure 3. Molecular representation of the three lowest energy conformers of xylobiose in its native (left) and modified form (right).

O-5 for the two lowest energy minima, and between O-3 and O-2 for the third one.

The adiabatic potential energy surface of xylobiose looks similar to those already reported for related disaccharides that are connected by β-(1→4)-linked di-equatorial glycosidic linkages: cellobiose[20] and mannobiose.[32] Differences are attributed to the absence of the hydroxymethyl group at C-5 in the xylobiose structure: it is expected that both steric hindrance and the potential to form inter-residues hydrogen bonds are lower. When compared with cellobiose and mannobiose, the total accessible area of xylobiose, encompassed by the upper contour limit seems larger; the two energy minima located within the main low energy area are closer in energy and are geometrically different in particular a shift along the ψ axis; the two minima of xylobiose differ by 80° and are separated by an energy barrier higher than 2 kcal/mol; the accessible space of the auxiliary region at *gauche*+, *gauche*−, is large for xylobiose and two minima appear; folded conformations are much more important for xylans than that for related molecules having an hydroxymethyl group at C-5; finally, a satellite at ϕ, ψ values *gauche*+, *gauche*+ has never been observed in other molecules.

3.1.2. Effect of substitution by fatty acid chains: Xyl23s-Xyl23s. Conformational behaviour of the substituted dimer graphically represented in the contour plot of Figure 2 (right), presents notable differences, when compared with the potential energy surface of xylobiose. The total accessible area is globally narrower than that observed for the native dimer, showing qualitatively that the substituted dimer is slightly more sterically restricted than its native counterpart. Exact positions of the lowest energy areas are displaced with respect to values observed for the nonsubstituted xylobiose. The lowest energy conformations are all aligned on a transversal axis going through ϕ, ψ (*gauche*+, *gauche*−); (*trans*, *trans*); (*gauche*−, *gauche*+). Geometric inspection of these models (Fig. 3 right) reveals that the two oxygen

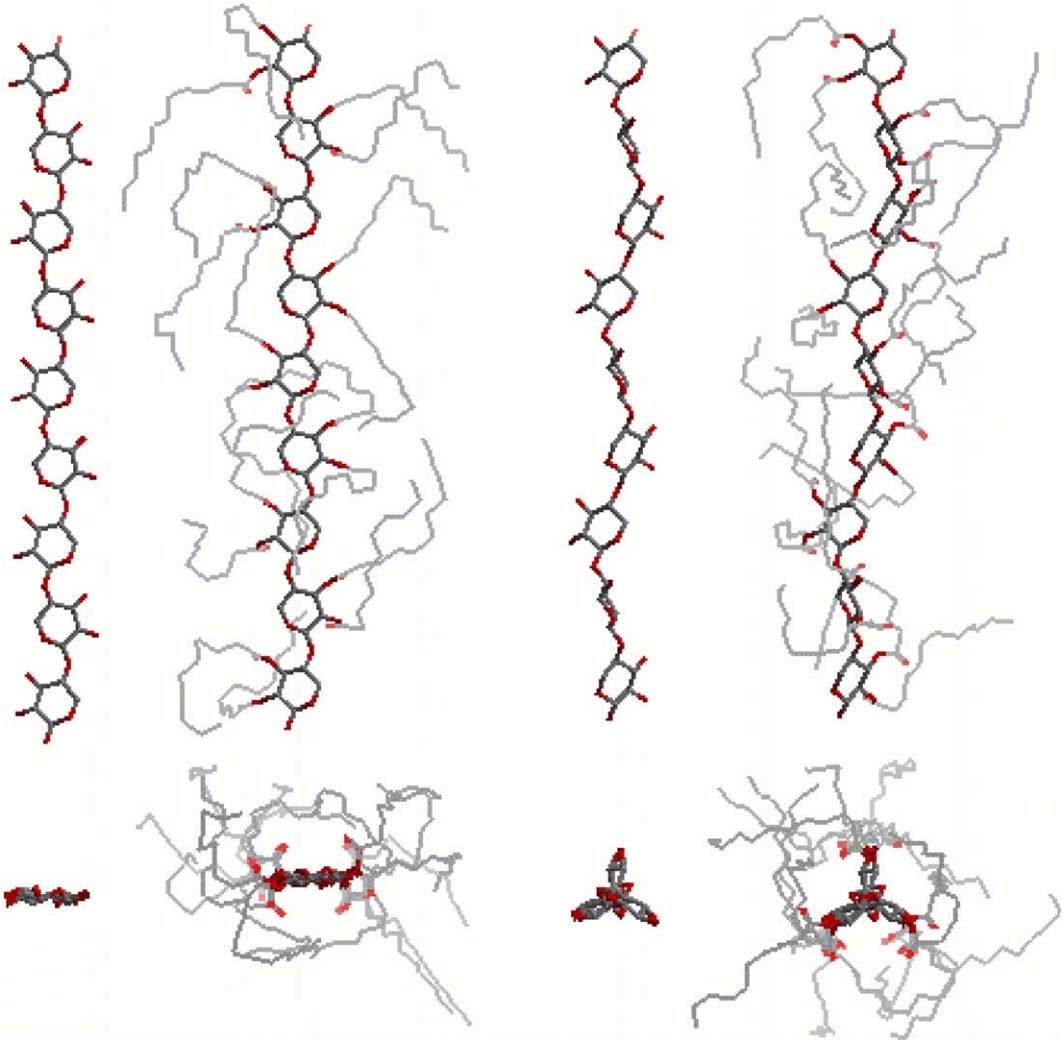

Figure 4. Side and top view of helices [11] 2_1 and [12] 3_1 in native and modified forms.

atoms O-2 and O-3 of both residues lie on the same side of the molecule, leading to favourable interactions between alkyl chains. Importantly, the zone corresponding to the extended conformations, which is the major area of native xylobiose corresponds only to minor conformations of the modified dimer. The relevance of the folded conformations is therefore increased and the conformational restriction depicted by the upper contour is counterbalanced by the presence of several energy minima that strongly differ in geometry but whose energy are comparable (Fig. 2).

3.2. Conformational behaviour of the polymer chains

3.2.1. Ordered conformations. Stereoregular helical conformations were extrapolated from the geometry of the low-energy regions of the potential energy maps of the two disaccharides, in addition to those proposed in the literature which model xylan in the crystal state.[9,10,30,31] Side and top views of selected helical forms of xylans are given in Figure 4. The corresponding helical (helices are characterized by two helical parameters n and h; n being the number of repeating units per turn of helix and h the projection of the repeating unit along the helical axis), structural, and energetic parameters are reported in Table 2. Only the stable predicted helices were considered for subsequent analysis.

In the present study, we considered helices having two to six residues per helical turn; results show that only the extended helices, having a pitch (h) between 10 and 15 Å, are favourable in energy. For both native and modified xylans, the left-handed 3_1 and 2_1 helices are the most stable; in the crystalline state, only 3_1 helices occur. Other helices: right-handed 3_1, 4_1, 5_1 and 6_1 are predicted higher in energy. Importantly, helices generated from the geometries of the predicted folded conformers of the disaccharides are not stable; this is related to the oligomer effect. The alkyl chains coat the xylan backbone in the modified structures (see Fig. 4); this is probably due to the fact that the molecular dynamics used to reveal the preferred orientations of the chains with respect to the backbone was performed in the absence of explicit surrounding molecules.

3.2.2. Disordered conformations. The hydrodynamic parameters and properties of native and modified xylans in solution have been gathered from statistical chains; the number of generated polymers, as well as the chain length were adjusted in order to get meaningful statistical data.

The polymer size is related to the persistence length (L_p) as a function of the DP whose variations for the native and substituted sample are given in Figure 5. The asymptotic limit of native polysaccharide persistence length is quickly reached, with $L_p = 35$ Å; such a value is characteristic of a semi-rigid polymer with moderate extension. Experimental determination of the persistence length of arabinoxylans gave values in the range 66–92 Å[33] whatever the substitution degree by arabinose side chains. These experimental data were recently reinterpreted to give an average value of 31 Å,[34] in excellent agreement with our predicted data. In addition, the predicted value is lower than those estimated for cellulose and mannan of about 100 Å, as observed experimentally.[35] As suggested by the conformational analysis of the dimers, lack of the hydroxymethyl group increases the accessible conformational space of the glycosidic

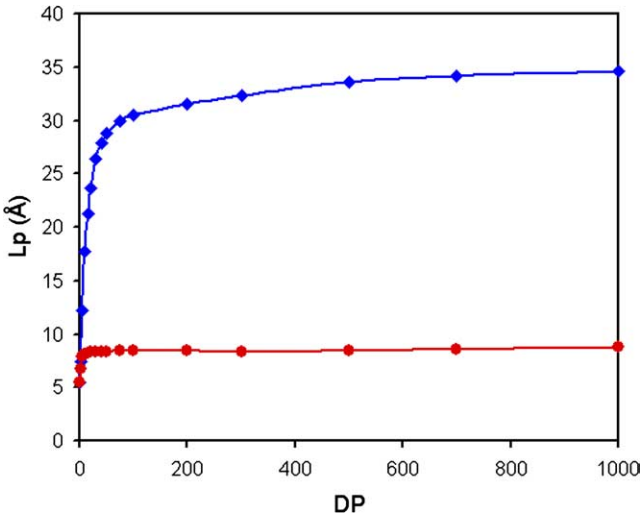

Figure 5. Persistence length L_p (Å) calculated as a function of the number of xylosyl residues, DP, of the simulated native xylan chain (blue) and the modified one (red).

Table 2. Helical, structural and energetic parameters of the helical conformations of native and substituted xylan build from the geometries of the proposed crystal structures of xylan and from the geometries of the energy minima of the disaccharides reported in Table 1

Helix	Chirality	n	H	ϕ (degree)	ψ (degree)	ΔE native xylan (kcal mol^{-1})	ΔE xylan 23s (kcal mol^{-1})
[1]	L	3	15.12	301	250	6	31
[7]	L	3	14.18	336	214	27	21
[8]	L	3	14.91	309	241	10	36
[9]	L	3	15.2	270	282	2	18
[10]	L	3	15.21	290	261	2	20
[11]		2	10.44	272	208	10	16
[12]	L	3	15.29	289	263	1	0
[20]	L	3	15.26	276	276	0	14

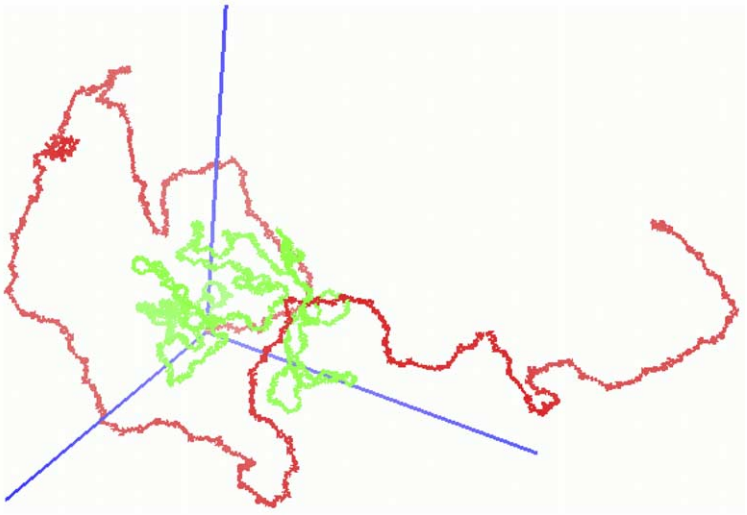

Figure 6. Snapshots of disordered chains of native (red) and modified (green) xylan. Axes lengths are 200 Å.

bonds, the corresponding polymer has a worm-like appearance. Chemical modifications of the polysaccharide considerably lower the predicted persistence length to the value of 9 Å, the corresponding structure is extremely compact.

A snapshot of typical polymer conformations having only 300 main chain units is given in Figure 6, illustrating the moderately extended and sinuous character of the native xylan polysaccharide and the collapsed coil of the modified xylan.

3.3. Amorphous solids

The polymer in an amorphous bulk state is represented as an ensemble of cubic microscopic structures for which periodic continuation conditions are employed. These microstructures are a part of an infinite medium that adequately model solids. The average predicted equilibrium densities are 0.920 ± 0.008 and 0.916 ± 0.012 g cm^{-3} for the native and modified forms respectively. The density of the crystalline xylan, estimated from the reported cell dimensions,[30] is 1.30 g cm^{-3}. As a general trend for polymers, the density of the amorphous phase is expected to be 20% lower than that of the crystalline phase. The density of the amorphous xylan should then be close to 1.0 g/cm^3. Our models agree well with this value (Fig. 7).

The cohesive energy is a widely used parameter for characterization of polymeric systems. It is defined as the ensemble average of the intermolecular part of the internal energy per mole of substance. The cohesive energy density corresponds to the cohesive energy per unit of volume and Hildebrand's solubility parameter, δ, is the square root of the cohesive energy density. Table 3 gives the averages of the cohesive energy densities and solubility parameters of each simulated system.

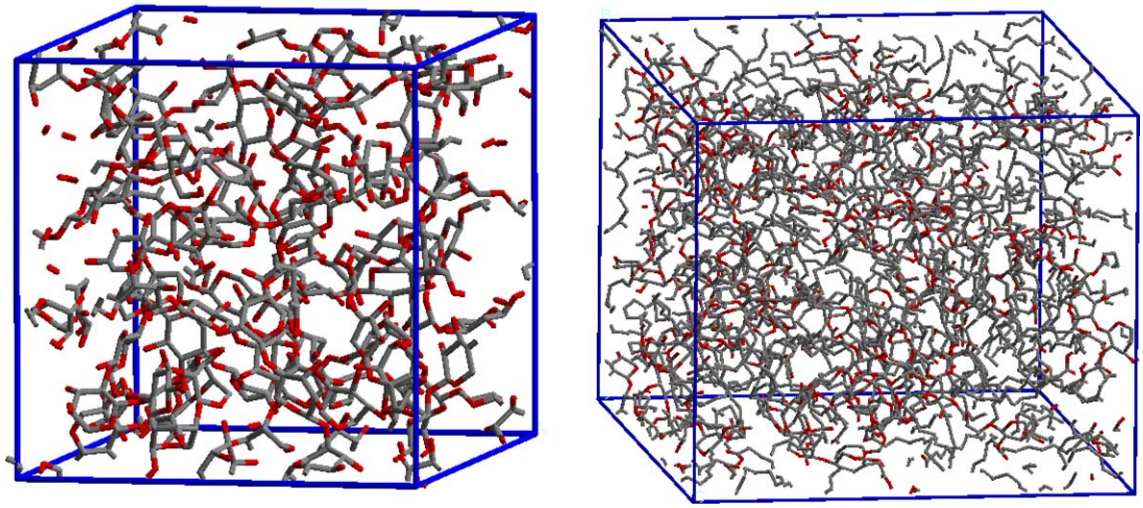

Figure 7. 'In cell' view of the amorphous solids: native structure (left), 23s structure (right).

Table 3. Cohesive energy densities (kcal/mol/cm^3) and solubility parameters ((J/cm^3)$^{1/2}$) for the native and modified forms of xylan

	CED	δ
Native xylan	0.108 ± 0.024	27.16 ± 3.09
Modified xylan	0.043 ± 0.051	15.55 ± 7.36

The cohesive energy density is dependent on the chemical substitution of the xylan chains; the computed systems display a large difference between the native and the modified xylans, the native polymer being the most stabilized by intermolecular interactions. This agreed well with T_g behaviour that decrease as flexible fatty chains are introduced, as a result of an increased spacing between polymer chains and dilution of secondary bonding, increasing the mobility of the xylan chains, which corresponds to a plasticization effect.

These parameters were estimated for cellulose by using the same methodology described in an earlier study,[19] a comparison between cellulose and xylan is then possible. In the amorphous state, the cohesive energy density of cellulose and its solubility parameter are 0.672 kcal/mol/cm^3 and $\delta = 68.33$ (J/cm^3)$^{1/2}$, respectively. Not surprisingly, as the hydroxymethyl group of cellulose is strongly involved in intermolecular interactions, values for the xylan polymer are considerably lower.

4. Conclusion

Substitution of xylan hydroxyl groups by lauroyl side chains has a considerable effect on the conformational properties of the chain. The potential energy surfaces of the dimeric model compounds differ together with the location of the lowest energy conformers. However, only extended helical conformations that resemble those found in crystal structures are predicted stable for both xylans. In contrast, unperturbed average dimensions of disordered chains are sensible to the presence of substituents, the native xylan chain is predicted semi flexible with moderate extension whereas the modified xylan behaves as a flexible coil. Condensed mechanically stable amorphous phases have also been generated. The predicted densities of these models are realistic and the estimated cohesive parameters show clearly that the native xylan is more stabilized by interchain interactions than that of the modified xylan. Some results of the present molecular modelling investigation are in accordance with both early theoretical approaches on related structures and by experimental measurements.

References

1. Ebringerova, A.; Hromadkova, Z. *Biotechnol. Genet. Eng. Rev.* **1999**, *16*, 325–346.
2. Chanliaud, E.; Saulnier, L.; Thibault, J. F. *J. Cereal. Sci.* **1995**, *21*, 195–203.
3. Fredon, E.; Granet, R.; Zerrouki, R.; Krausz, P.; Saulnier, L.; Thibault, J. F.; Rosier, J.; Petit, C. *Carbohydr. Polym.* **2002**, *49*, 1–12.
4. Moine, C.; Gloaguen, V.; Gloaguen, J.-M.; Granet, R.; Krausz, P. *J. Environ. Sci. Health, Part B* **2004**, *B39*, 627–640.
5. Jain, R. K.; Sjostedt, M.; Glasser, W. G. *Cellulose* **2000**, *7*, 319–336.
6. Warth, H.; Mulhaupt, R.; Schatzle, J. *J. Appl. Polym. Sci.* **1997**, *64*, 231–242.
7. Wang, P.; Tao, B. Y. *J. Appl. Polym. Sci.* **1994**, *52*, 755–761.
8. Gabrielii, I.; Gatenholm, P. *J. Appl. Polym. Sci.* **1998**, *69*, 1661–1667.
9. Sundararajan, P. R.; Rao, V. S. R. *Biopolymers* **1969**, *8*, 305–312.
10. Rees, D. A.; Skerrett, R. J. *Carbohydr. Res.* **1968**, *7*, 334–348.
11. Ebringerova, A.; Heinze, T. *Macromol. Rapid Commun.* **2000**, *21*, 542–556.
12. Allinger, N. L.; Rahman, M.; Lii, J. H. *J. Am. Chem. Soc.* **1990**, *112*, 8293–8307.
13. Allinger, N. L.; Yuh, Y. H.; Lii, J. H. *J. Am. Chem. Soc.* **1989**, *111*, 8551–8566.
14. Maple, J.; Dinur, U.; Hagler, A. T. *Proc. Nat. Acad. Sci. U.S.A.* **1988**, *85*, 5350–5354.
15. Maple, J. R. *Israel J. Chem.* **1994**, *34*, 195–231.
16. Maple, J. R.; Hwang, M. J.; Stockfisch, T. P.; Dinur, U.; Waldman, M.; Ewing, C. S.; Hagler, A. T. *J. Comput. Chem.* **1994**, *15*, 162–182.
17. Sun, H. *Macromolecules* **1995**, *28*, 701–712.
18. Sun, H.; Mumby, S. J.; Maple, J. R.; Hagler, A. T. *J. Am. Chem. Soc.* **1994**, *116*, 2978–2987.
19. Mazeau, K.; Heux, L. *J. Phys. Chem. B* **2003**, *107*, 2394–2403.
20. French, A. D.; Dowd, M. K. *Theochem* **1993**, *105*, 183–201.
21. Engelsen, S. B.; Cros, S.; Mackie, W.; Perez, S. *Biopolymers* **1996**, *39*, 417–433.
22. Perez, S.; Delage, M. M. *Carbohydr. Res.* **1991**, *212*, 253–259.
23. Flory, P. J. *Stat. Mech. Chain Molecul.* **1969**, 432pp.
24. Metropolis, N.; Rosenbluth, A. W.; Rosenbluth, M. N.; Teller, A. H.; Teller, E. *J. Chem. Phys.* **1953**, *21*, 1087–1092.
25. Boutherin, B.; Mazeau, K.; Tvaroska, I. *Carbohydr. Polym.* **1997**, *32*, 255–266.
26. Pricl, S.; Lapasin, R., (Eds.); *Rheology of Industrial Polysaccharides: Theory and Applications*; 1995; 640pp.
27. Verlet, L. *Phys. Rev.* **1967**, *159*, 98–103.
28. Parrinello, M.; Rahman, A. *J. Appl. Phys.* **1981**, *52*, 7182–7190.
29. Nosé, S. *Mol. Phys.* **1984**, *52*, 255–268.
30. Nieduszynski, I. A.; Marchessault, R. H. *Biopolymers* **1972**, *11*, 1335–1344.
31. Sundararajan, P. R.; Marchessault, R. H. *Can. J. Chem.* **1975**, *53*, 3563–3566.
32. Petkowicz, C. L. O.; Reicher, F.; Mazeau, K. *Carbohydr. Polym.* **1998**, *37*, 25–39.
33. Dervilly-Pinel, G.; Thibault, J. F.; Saulnier, L. *Carbohydr. Res.* **2001**, *330*, 365–372.
34. Picout, D. R.; Ross-Murphy, S. B. *Carbohydr. Res.* **2002**, *337*, 1781–1784.
35. Swenson, H. A.; Schmitt, C. A.; Thompson, N. S. *J. Polym. Sci., Part C: Polym. Symp.* **1965**, 243–252.